



# CAVITATION MODELS FOR STRUCTURES EXCITED BY A PLANE SHOCK WAVE

K. MÄKINEN

*Karlskronavarvet AB, S-371 82 Karlskrona, Sweden*

*and*

*Royal Institute of Technology, Department of Aeronautics, Division of Lightweight Structures  
S-100 44 Stockholm, Sweden*

(Received 28 November 1995 and in final revised form 30 July 1997)

The response of submerged structures to an underwater explosion generally involves the nonlinear behaviour of the fluid and/or the structure. The modelling of such systems would be very difficult; however, simplifications can be made in which the representation of the effect of the fluid on the structure requires special consideration. The Plane Wave Approximation (PWA) is used to represent the fluid during the early shock-loading phase of the analysis and four different models are compared for modelling the cavitation when the pressure at the structure falls below the cavitation pressure. A simple method is provided to study the effects of different parameters, concerning the cavitation, in this very complex problem. Closed-form solutions provide the basis of comparison for the validation of the PWA approach, example problems are presented, including the shock response of plates, and the results from the different cavitation models are compared. © 1998 Academic Press Limited

## 1. INTRODUCTION

WHEN IT COMES to the design of military vessels exposed to underwater explosions the resistance against a shock wave is of major concern. The shock analysis of a vessel involves several aspects, such as (a) the arrival of the initial shock wave, (b) the decay of the initial shock wave, (c) local cavitation due to the surface-reflected shock wave or the structural reflected shock wave, (d) fluid–structure interaction, (e) local cavitation collapse, and (f) structural response. The whole sequence of events leads to a problem which is quite complicated and difficult to predict. For simple geometries, closed-form solutions can be found; but for practical structures, numerical methods are unavoidable. However, even the numerical solution of the coupled governing equations becomes intractable for structures with hundreds of degrees of freedom. Therefore, approximate methods have been developed to solve the fluid–structure interaction problem (Felippa & Deruntz 1984) for the early-time solution. The methods utilize the plane wave approximation (PWA) which is an approximation for the early stages of the response and was first developed by Mindlin & Bleich (1953). The method has been used extensively by Geers (1974) for the early-time predictions of the response of surface ships and submarines exposed to underwater explosions. For surface vessels, the effect of cavitation can be significant and commonly used models for the phenomena are the displacement criteria, DiMaggio *et al.* (1981), and the pressure criteria, Moyer *et al.* (1992). These are very simplified models for a very complex phenomenon to which there is not yet a unique solution. Both Driels (1980) and Handleton (1985) have

investigated this problem, and Driels included the effect of nonzero cavitation pressure. To calculate the cavitation closure pressure they use a model where the cavitated water is segmented into a number of elements which, when the cavity closes, starts to load the structure. In 1982 Mørch (1982) developed a theory and closed-form solutions for the growth and collapse of one-dimensional cavitation clusters at a rigid wall and later (Mørch 1989) for a spherical cavity cluster. When the cavitation closes, the reloading causes an impact pressure on the structure, and the same function as for the initial shock wave is commonly used, as by Moyer *et al.* (1992). However, the reloading is a different physical phenomenon from the initial shock wave and a slamming model developed by Chaung (1966) has been used in this paper.

In the numerical examples, expressions from Cole (1948) are used to determine the incident pressure from the explosive charge. The pressure is affected by the reflecting of the incident wave in the water surface and the point-source imaging technique is used to calculate the arrival time of the reflected wave. The growth and collapse of the cavitation at the fluid–structure interface is represented either by the displacement or pressure criteria or by theories developed by Mørch. The alternative function by Chaung, as well as the initial function, for the reloading of the structure after cavitation is investigated. The problems have been solved with a combination of the Runge–Kutta method with adaptive step-size control to solve the cavitation models developed by Mørch and the finite element method using the plane wave approximation for the structural response.

## 2. THEORY

### 2.1. PLANE WAVE APPROXIMATION

Since the loading on the structure and the motion of the boundary are linked together, the structural and fluid equations cannot be solved separately. The motion of a structure, discretized into a finite element mesh, is given by the differential matrix equation

$$M\ddot{x} + C\dot{x} + Kx = F(t), \quad (1)$$

where  $M$  is the structural mass matrix,  $C$  the structural damping matrix,  $K$  the structural stiffness matrix,  $x$  the structural displacement, the dot denoting differentiation with respect to time, and  $F(t)$  the time-varying load applied to the structure.

By superimposing an imaginary fluid mesh on the fluid–structure boundary, the surface-force compatibility on the submerged structure can be written as

$$F(t) = -GA_f(p_i + p_s), \quad (2)$$

where  $G$  is the matrix relating the structural degrees of freedoms to those of the fluid,  $A_f$  the matrix containing the areas of “the elements” in the fluid mesh,  $p_i$  the incident (direct) pressure from the underwater explosion, and  $p_s$  the scattered pressure from the structure, i.e. part of the pressure hitting the structure that is reflected back into the fluid.

Compatibility at the fluid–structure interface in the normal direction requires that the surface-normal-velocity of the structure and fluid are equal, i.e.

$$G^T \dot{x} = v_i + v_s, \quad (3)$$

where  $v_i$  is the incident water particle velocity from the underwater explosion, and  $v_s$  the scattered water particle velocity from the structure.

The fluid is considered to be inviscid and incompressible, i.e. the density changes are infinitesimally small compared to the initial value. The scattered acoustic pressure and scattered fluid particle velocity are related by

$$p_s = \rho c v_s, \quad (4)$$

where  $\rho$  is the water density, and  $c$  the speed of sound in water.

The equation for the early time can be derived by rearranging equation (3) and substituting into (4):

$$p_s = \rho c (G^T \dot{x} - v_i);$$

the resulting expression for  $p_s$  is then substituted into equation (2) and an expression for the load  $F(t)$ , is obtained:

$$F(t) = -GA_f [p_i + \rho c (G^T \dot{x} - v_i)].$$

$F(t)$  is finally substituted into equation (1) to obtain the differential equation for the early-time response of a structure,

$$M\ddot{x} + (C + GA_f G^T \rho c)\dot{x} + Kx = -GA_f (p_i + \rho c v_i). \quad (5)$$

The term  $\rho c$  represents an additional damping term to the structure; it is due to the energy radiated away from the structure into the fluid. A loading term arises from the incident particle velocity. The only unknown term in equation (5) is the structural displacement  $x$ . This equation can easily be solved by using almost any of the available computer codes based on the finite element method.

## 2.2. CAVITATION MODELS

### 2.2.1. Displacement criterion (DC)

Cavitation, in the displacement criterion (DC) and the other models, is assumed to start when the total pressure in the fluid becomes negative, or when structural and fluid nodes separate, at time  $t_1$ . For a structure near the surface this often occurs when the surface-reflected wave reaches the actual point under consideration. The total pressure at a point,  $p_T$ , is defined as

$$p_T = (p_i + p_r) + p_s + p_h, \quad (6)$$

where  $p_i$  is the incident pressure,  $p_r$  is the reflected pressure, and  $p_h$  the hydrostatic pressure.

The scattered pressure,  $p_s$ , is simply calculated from the difference between the incident water particle velocity and the structural velocity. The reloading for the DC occurs when the displacement between the structural and fluid node returns to zero again, i.e. at a time  $t_2$  when the condition in equation (7) is satisfied:

$$\int_{t_1}^{t_2} (\dot{x} - v_f) dt = 0, \quad (7)$$

where  $v_f$  is the fluid velocity.

### 2.2.2. Pressure criterion (PC)

The cavitation starts, as for the DC, when the total pressure equation (6) becomes negative or when the structural and fluid nodes separate. The loading is applied again when the surrounding pressure,  $p_\infty$ , becomes positive:

$$p_\infty = (p_i + p_r) + p_a + p_h, \quad (8)$$

where  $p_\infty$  is the surrounding pressure, and  $p_a$  the atmospheric pressure.

By replacing the scattered pressure with the atmospheric pressure, equation (6) leads to an expression for the surrounding pressure during cavitation. This is permitted because there is no scattered pressure from the structure during cavitation, since there is a cavity between the structure and the fluid. In this criterion it is assumed that there is zero pressure in the cavity and therefore the atmospheric pressure must be added to the surrounding pressure.

Compared with the DC, the pressure criterion (PC) is more realistic because the reloading is expected to occur slightly earlier in time than the cavitation models described in Sections 2.2.3 and 2.2.4, i.e. when the surrounding pressure becomes positive.

A cavity in the cavitation models grows during the time when the surrounding pressure is less than zero. During this time the water is displaced and will obtain a certain amount of potential energy relative to its state of equilibrium. When the surrounding pressure becomes positive, the cavity starts to collapse and the energy in the displaced water is released and will make the collapse time much shorter. The reloading is expected to occur slightly after the surrounding pressure becomes positive for the cavitation models.

### 2.2.3. Rigid wall model (RWM)

A cavitation model for a one-dimensional cluster at a rigid wall has been developed by Mørch (1982) and is used to describe the growth and collapse of the cavity caused by the underwater explosion. The governing equation is as follows:

$$\ddot{y}(h - \beta y_0 - (1 - \beta)y) - \dot{y}^2(1 - \beta)\frac{1}{2} = -(p_\infty - p_v)/\rho\beta, \quad (9)$$

where  $y$  is the thickness or radius of cavity, the dot denoting differentiation with respect to time,  $h$  the depth under water surface,  $\beta$  the fraction of cavities, typically in the order of 0.01–0.1 ( $\beta = 1$  indicates a fully developed cavity),  $y_0$  the initial cavity thickness, and  $p_v$  the vapour pressure.

The governing equation (9) is developed for a rigid wall model (RWM), but in this case the solution is super-imposed on the structural solution, which means that the “rigid wall” is actually moving.

When the cluster shrinks, potential energy is first converted into kinetic energy of the flow of liquid towards the cluster boundary and then into wave energy as the individual cavities are annihilated at the boundary. The wave energy is partly radiated from the cluster and lost, and partly radiated into the cluster again and then converted into kinetic energy of the further collapse of the cluster. During the collapse, the velocity in the fluid is a function of time only,

$$v_f = \beta\dot{y}. \quad (10)$$

At the moment when the boundary of the cavity layer reaches the plate the fluid impacts the plate with velocity ( $v_f$ ) and an impact peak pressure ( $p_0$ ) is developed:

$$p_0 = \rho c v_f = \rho c \beta \dot{y}, \quad (11)$$

where  $p_0$  is the peak pressure.

#### 2.2.4. Single spherical cavity model (SCM)

Mørch (1989) also developed an expression for the growth and collapse of a single spherical cavity model (SCM) and has the following form:

$$y\ddot{y} - 3\dot{y}^2/2 = -(p_\infty - p_v)/\rho\beta. \quad (12)$$

If  $\beta = 1$  this equation takes the form of the Rayleigh–Plesset equation. This equation cannot be used directly because it describes a spherical wave rather than a plane wave. However, if the radius of the sphere is large enough, it may be considered as plane for a small portion of the sphere. By assuming an initial radius of two times the circumference of the area associated with the fluid node, we may consider the spherical wave as a plane wave. When assuming this initial radius, the small portion of the sphere does not differ by more than 2% from a plane surface. By letting the cavity grow from and collapse to this initial radius, the velocity at the boundary of the fluid can be obtained:

$$y_0 = 4\sqrt{\pi A_f}. \quad (13)$$

Similarly to the RWM the fluid velocity can be obtained from the solution of equation (10) and the impact pressure on the structure from equation (11).

### 3. LOAD PRESSURE

#### 3.1. INCIDENT PRESSURE FROM AN EXPLOSIVE CHARGE

From an underwater shock explosion, the shock pressure can be calculated according to Cole's (1948) formula:

$$p_i = p_0 \bar{e}^{t/\theta}, \quad (14)$$

where  $p_0$  is the peak pressure, given by  $p_0 = 56.6 (Q^{0.33}/R)^{1.15}$  in MPa,  $\theta$  is the decay constant, given by  $\theta = 0.084 \cdot Q^{0.33} (Q^{0.33}/R)^{-0.23}$  in ms,  $Q$  is the weight of explosive in kg,  $R$  the distance between point and charge in m, and  $t$  the time.

This relation is an approximation of the initial portion of the pressure curve from an underwater explosion, and the constants  $p_0$  and  $\theta$  are empirical values for HBX charges (HBX is a type of explosive).

This expression is valid for the loading before the “surface cut-off” occurs and is also commonly used for reloading after cavitation. However, physically we are concerned with two different phenomena. In the first case, the structure and the fluid are in contact with each other when the shock wave starts to act on the system. In the second case, both the fluid and structure are moving separately and the difference in velocity (at the instant of reloading) is causing the loading on the structure. A better way to describe this phenomenon would perhaps be to use some model for slamming loads.

### 3.2. EFFECTS ON THE INCIDENT PRESSURE

The effect of a free surface is very important to a surface ship. When the direct wave “hits” the surface it is reflected and it changes sign. This means, if we are looking at a point on the structure, it is first going to be hit by the incident (direct) wave and a short time later, depending on the distance the wave has to travel, a reflected wave from the water surface. The distances are easily calculated from the explosion geometry, using the imaging technique, as shown in Figure 1. This reflected wave will cancel out the incident wave and we will get what is called the “surface cut-off”. A typical pressure curve is shown in Figure 2.

In Figure 2, one can observe the typical events in the pressure from an underwater explosion. First, we have the arrival of the initial shock wave with an instantaneous pressure increase, followed by the exponential decay described by equation (14). Then follows the “surface cut-off” due to the arrival of the surface-reflected wave and a long cavitation period. Then, as indicated in Figure 2, depending on what model is used for the cavitation, the reloading of the structure may occur at different times.

Since the water cannot withstand any significant amount of tension (in the order of 10–100 kN/m<sup>2</sup> for very short times) the cavitation will start at the time when the total pressure,  $p_T$ , is less than the maximum tension. The pressure inside the cavity will be the vapour pressure (at 7°C it is equal to 1.0 kN/m<sup>2</sup>, but for practical applications zero is often used). The driving pressure for the growth of the cavity will be the difference between the surrounding pressure outside the cavity in the fluid and the vapour pressure inside the cavity. As long as this pressure is less than zero the cavity will grow. When the surrounding pressure becomes positive, the cavity starts to collapse and the reloading for the cavitation models occurs when the cavity has collapsed.

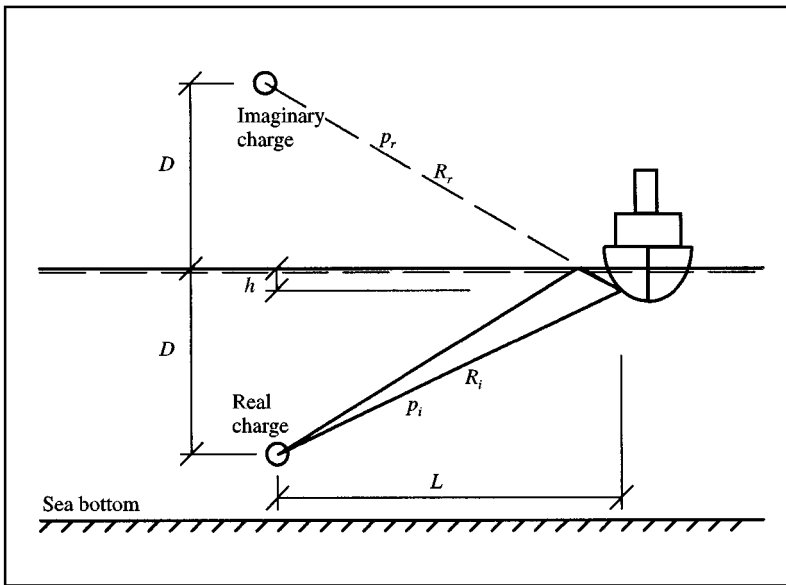


Figure 1. Imaging technique using real and imaginary charges;  $R_i$  = distance to real charge,  $R_r$  = distance to imaginary charge.

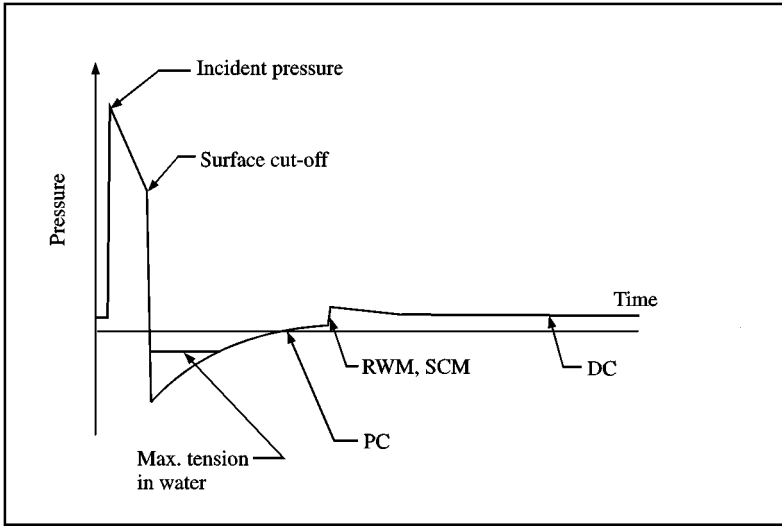


Figure 2. Typical pressure curve from an underwater explosion with “surface cut-off”, indicating reloadings in time.

### 3.3. SLAMMING PRESSURE

The same function is often used for the reloading and the initial shock wave; this is not completely correct since we are looking at two different physical phenomena. When the initial shock wave hits the structure, the fluid is in contact with the structure and it is a pressure increase that causes the load. At reloading, the structure and fluid are separated and it is the impact of the fluid on the structure that is causing the load. If one adopts this second approach, the event is more like a slamming load. Chuang (1966) performed an experimental investigation of the rigid flat-bottom slamming phenomena. On the basis of these experiments a set of equations was derived to predict the impact pressure of a rigid flat-bottom body slamming, namely

$$p_i = 2p_0 e^{-1.4t/T} \sin(\pi t/T), \quad (15)$$

where  $p_0$  is the peak pressure, with  $v_f$  in m/s:

$$p_0 = 0.1v_f, \text{ in MPa,}$$

$T$  is the duration of the first pulse, with  $A_f$  in  $\text{m}^2$ :

$$T = 24.5 \sqrt{A_f/c_{\text{air}}} \text{ in s,}$$

and  $c_{\text{air}}$  is the speed of sound in air, in m/s.

It is generally believed that flat-bottom slamming is a combined acoustic and hydrodynamic phenomenon. From experiments with cavitation and flat-bottom slamming, there is trapped air at the interface between the structure and the fluid. Because of this similarity, the approach of using this slamming function is not completely wrong. Both the expressions for the initial shock pressure and the slamming pressure are empirical formulae,

and there are a number of local phenomena that are not accounted for and are not looked into any further.

## 4. NUMERICAL MODEL

### 4.1. FINITE ELEMENT MODEL

In the finite element modelling, the plane wave approximation is used to characterize the fluid behaviour during the early time of the shock pulse from an explosion. As shown in Figure 3, a simple one-dimensional model of a structure including the fluid–structure interface, fluid node and structural stiffness can be developed.

The fluid damper is a result of the vibration energy being lost by structural work on the fluid, which is acoustically transmitted away from the structure. In this simple one-dimensional problem with a unit area and when considering the sign on the incoming and reflected fluid particle velocity, equation (5) reduces to

$$M\ddot{x} + \rho c\dot{x} + Kx = -2p_i. \quad (16)$$

The model according to equation (16) is valid for the early-time response of a structure and without structural damping. Based on this simple one-dimensional fluid–structure model, one can identify three phases in the loading and response of the system, as follows.

*Phase I:* Application of the shock load to the fluid node. This results in a change of velocity of the structure. The structure and fluid move according to an acoustic plane wave.

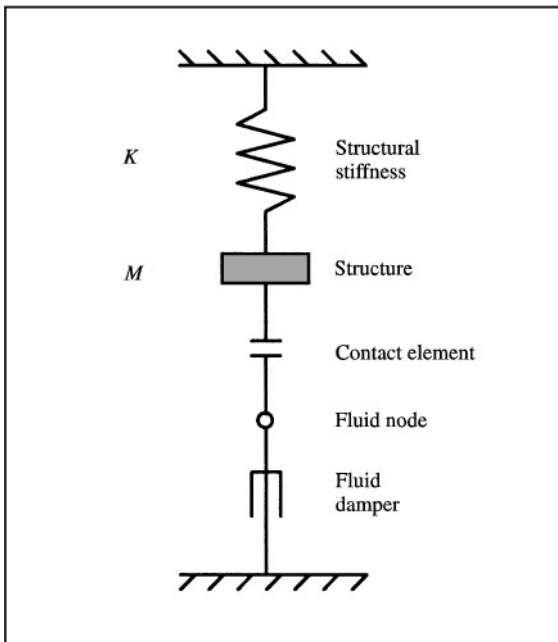


Figure 3. Model for a fluid–structure interaction between a structure and a fluid surface.



*Phase II:* For all the models, cavitation occurs either when the total pressure becomes less than zero or when the displacement between the structural and fluid node is greater than zero. On the structure, the atmospheric pressure, gravity forces and structural stiffness act to close the cavity. Different forces act on the fluid node, depending on which cavitation criteria or model is used.

*Phase III:* The structure and fluid come in contact with each other again. This reloading may result in forces on the structure which are comparable to the initial forces from the shock-pulse. When this occurs, the strength of the impact is dependent on which model is used to represent the cavitation in the fluid at the fluid–structure interface.

#### 4.2. CAVITATION MODELS

Atmospheric and gravity forces are present on the structure for all the cavitation models during cavitation. In the DC the incident, reflected, atmospheric and hydrostatic pressures are acting on the fluid node, equation (8). Equation (7) starts acting when cavitation begins and indicates when the shock load is to be applied to the fluid node again, that is when the structure and fluid are in contact again. In the PC, equation (8) acts as a switch; when it becomes positive reloading occurs. In both the DC and PC no additional load is applied to the structure due to the impact of the fluid on the structure.

In the RWM of the cavitation, equation (9) is solved for every time-step in the analysis of the structure from the beginning of cavitation and controls the size of the cavity between the structure and fluid. When the size of the cavity becomes zero, the reloading is introduced to the system. In the SCM, equation (12) governs the size of the cavity between the structure and fluid. This equation is also solved at every time-step after cavitation has occurred in the analysis. However, in this case there must be an initial size of the cavity according to equation (13), from which the cavity will grow and collapse to, before the reloading is applied to the system. For both the RWM and SCM the fluid velocity is obtained from equation (10) and the pressure on the structure at impact from equation (11).

### 5. NUMERICAL EXAMPLES

Since there are a number of parameters in equations (9) and (12) for the two cavitation models, RWM and SCM, an investigation was first made to see the difference in the fluid velocity ( $v_f$ ) using different parameters. In all the problems in this section, the Runge–Kutta method is used for solving the cavitation equations and the finite element method to solve the structural equation. In the transient problem that need to be solved, a time step of 0.1 ms is used.

The vapour pressure,  $p_v$ , was set to either 0 or 1000 Pa, the surrounding pressure,  $p_\infty$ , to  $-0.01$ ,  $-0.05$  or  $-0.10$  MPa to make the cavity grow and either 0.10 or 0.15 MPa to make the cavity collapse. Furthermore, the volume fraction of cavities,  $\beta$ , was set to 0.01, 0.05, 0.10, 0.50 or 1.00.

Based on the calculations it was found that both the difference in vapour pressure and volume fraction of cavities,  $\beta$ , had very little influence on the fluid velocity: less than 3%. The closure of the cavitation occurred almost at the same time for the two cavitation models. Also, decreasing the surrounding pressure for opening the cavity will increase the fluid velocity at closure. A lower pressure gives a larger cavity, which in turn causes a greater

closure velocity and a longer time to closure. A higher pressure at cavitation closure, using the above values, decreases the fluid velocity and the time to closure.

The major difference in the fluid velocity is obtained by choosing between the RWM and SCM models and the surrounding pressure for cavitation growth. By using the two models and evaluating the fluid velocity for  $\beta = 0.05$ ,  $p_v = 0.001$  MPa, and  $p_\infty = -0.05$  MPa at cavitation growth and 0.15 MPa at cavitation closure, the curves indicated in Figures 4 and 5 are obtained. In Figure 4, an initial radius of 7.09 m (circumference of  $2A_f$ , with  $A_f = 1$ ) was used for the SCM.

The effect of the initial radius was investigated for the SCM as well. The fluid velocity was calculated with different radii between 1 and 3 times the circumference of the area

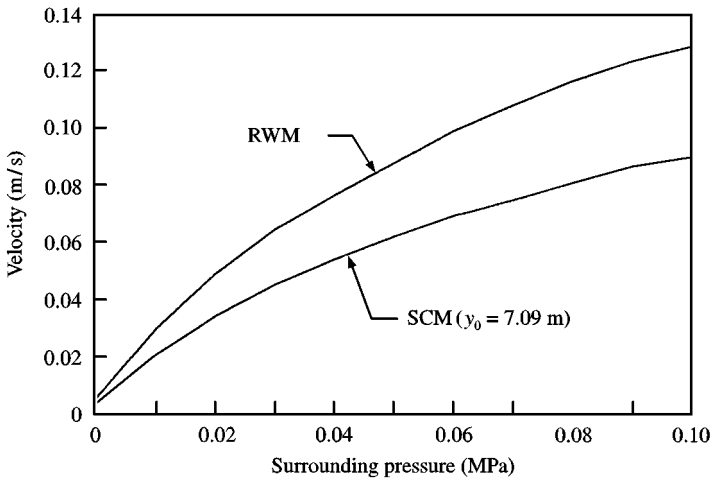


Figure 4. Fluid velocity of rigid wall model (RWM) and single spherical cavitation model (SCM).

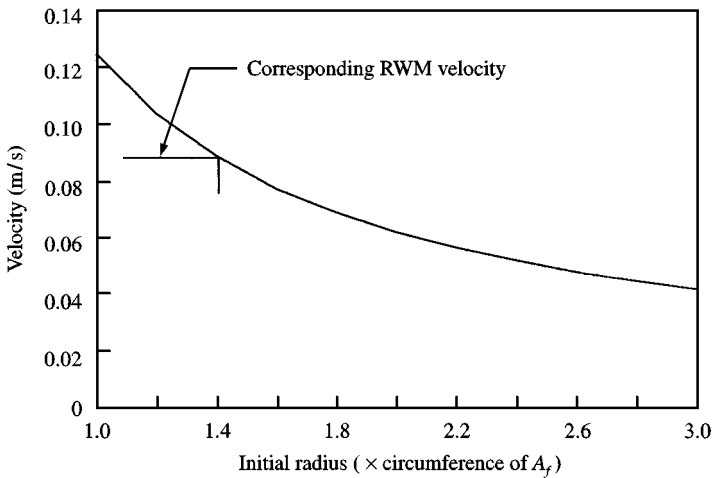


Figure 5. Fluid velocity as function of initial radius for single spherical cavitation model (SCM).

$A_f$  associated with the fluid node; the result is shown in Figure 5. As indicated in Figure 5, a radius of about 1.4 times the circumference of the area associated with the fluid node corresponds to the RWM.

If one particular point at a structure is considered, the growing pressure for the cavity can be chosen to be everything between zero and several MPa below zero. This is entirely dependent on how much tension the water can withstand; however, this parameter is very difficult to predict, but the figure is usually greater than the negative pressure caused by the underwater explosion. The closure pressure is dependent on the atmospheric pressure and the depth in the water. Therefore it is a fixed pressure for every particular point. If we are looking at the pressure from the underwater explosion at this stage, the explosion pressure is small due to its decay in time. This means that during cavitation, the pressure in the fluid from the underwater explosion can be ignored.

### 5.1. EXAMPLE 1: INFINITE PLATE BY TAYLOR (1941)

To illustrate the DC, a 6.35 mm thick infinite steel plate analytically solved by Taylor (1941), with density  $7874 \text{ kg/m}^3$  is analysed. The plate is subjected to a shock pulse from a 100 kg (HBX charge) at a distance of 15.25 m; the pulse falls to half its value in 0.3 ms, which gives  $p_0 = 1.55 \text{ N/m}^2$  and  $\theta = \frac{1}{2300} \text{ s}$ . Furthermore, the density of the water ( $\rho$ ) is assumed to be  $1000 \text{ kg/m}^3$  and the speed of sound in water ( $c$ ) is set to 1400 m/s. The restoring force is such that the plate has a free period of 0.01 s when not in contact with water.

The solution of equation (16) shown in Figure 6 is in very good agreement with Taylor's results, the maximum structural displacement occurs after 2.5 ms and is 28 mm, according to Taylor. The time-displacement curves for the structural and fluid nodes are shown in Figure 6(a).

Due to the shock pulse, an initial impulse (applied at the fluid node, see Figure 3) is given to the plate and the fluid, and it is likely that, at some stage, the fluid and plate will separate due to the inertia of the plate and the impulse given to the fluid. At this stage a tensile force would be required to hold the plate and fluid together, but the contact element opens up, representing the fact that the fluid cannot withstand any significant amount of tension. The restoring force acting on the plate forces the plate back to its initial position. The plate hits the fluid on the way back and the motion will be damped due to the  $\rho c$  damper, and the displacement will eventually return to zero. During the period after 4.5 ms, the plate and fluid follow the same pattern so that the velocity and acceleration becomes small.

The analysis is physically meaningful from the standpoint that a certain amount of energy is given to the plate before "cavitation", and since no energy is lost during "free flight" one expects the velocity of return to the fluid to be quite similar to the velocity of the plate when separation occurred. Furthermore, it can be seen in Figure 6(b) that the velocity is zero where the displacement in Figure 6(a) has its maximum, which also is physically correct.

### 5.2. EXAMPLE 2: INFINITE PLATE BY DiMAGGIO *ET AL.* (1981)

This is also a one-dimensional problem, but the loading function contains all the parts that a three-dimensional analysis would contain. The initial shock peak with surface cut off, a long cavitation period followed by cavitation closure with a second shock

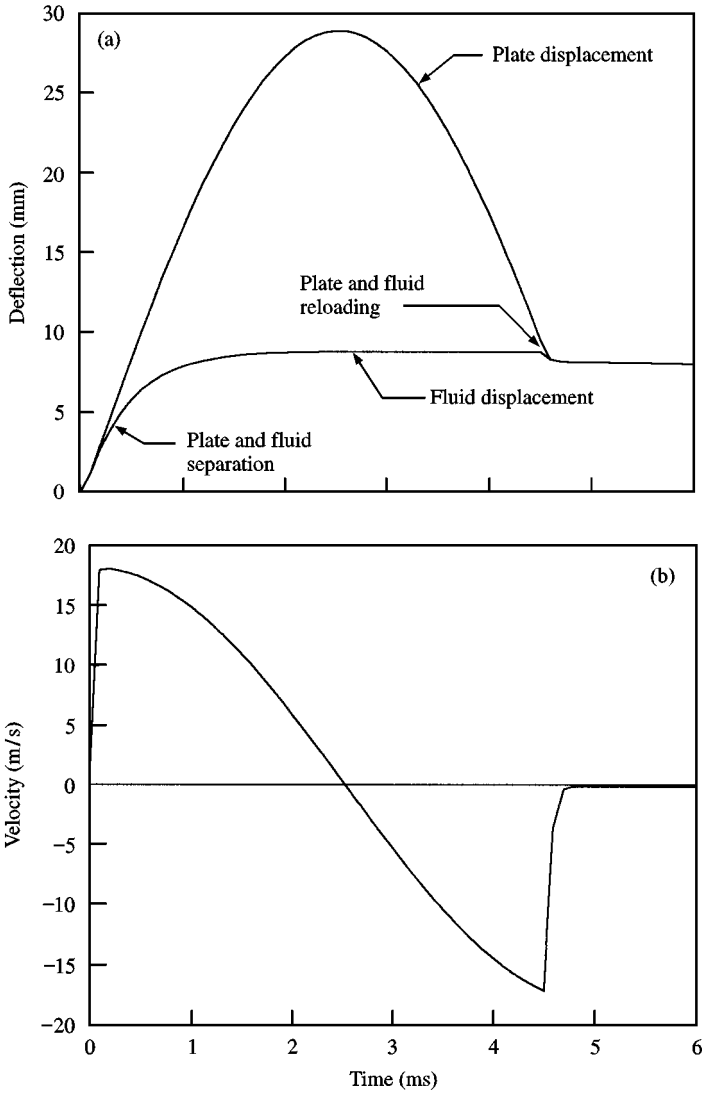


Figure 6. (a) Plate and fluid displacement time history; (b) plate velocity time history.

wave is included in the analysis. A mathematical model for the cavitation developed by Bleich & Sandler (1970) was used in the reference. This example is evaluated using all the cavitation models DC, PC, RWM and SCM, as described in Sections 2.2 and 4.2.

The following material and geometrical parameters were assumed:  $M = 4893$  kg;  $g = 9.81$  m/s<sup>2</sup>,  $c = 1524$  m/s,  $\rho = 1000$  kg/m<sup>3</sup>,  $A_f = 1$  m<sup>2</sup>,  $p_0 = 0.786$  MPa,  $\theta = 0.004$  s,  $p_a = 0.101$  MPa, and  $T = 0.0022$  s. Even though this is a one-dimensional problem, a cut-off time  $T$  is included, as an exercise, to model the sudden reduction in pressure associated with surface reflection of the incident wave. Using the expressions in equation (14) and the values of  $p_0$  and  $\theta$ ,  $Q$  and  $R$  can be evaluated as  $Q = 9088.5$  kg and  $R_i = 834.5$  m. Then, by

TABLE 1  
Summary of response for infinite for infinite plate by DiMaggio *et al.*

Cavitation Model	Cavitation		Reloading		Maximum displacement	
	Start (s)	Time (s)	Fluid vel. (m/s)	Plate vel. (m/s)	Time (s)	Plate defl. (mm)
DC	0.0022	0.0208	0.10	-0.15	0.0146	2.77
PC	0.0022	0.0054	0.16	0.28	0.0182	2.94
RWM	0.0022	0.0116	0.060	0.09	0.0204	3.04
SCM	0.0022	0.0116	0.045	0.09	0.0194	2.95

using the cut-off time  $T$ , a distance to the imaginary charge can be found and we obtain  $R_r = 837.9$  m. How well these values represent a real case could be questioned.

With  $\beta = 0.05$ ,  $p_v = 0.001$  MPa, and  $p_\infty = -0.05$  MPa for cavitation growth and 0.148 MPa for cavitation closure, the maximum acceleration in all models occurred at the first load step and was  $264.2$  m/s<sup>2</sup>; the other results are summarized in the Table 1.

From Table 1 it can be seen that the maximum displacement occurs after reloading for all models except for the DC and that the displacements are of the same order for all the models, but do not occur at the same time. In this example we have a heavy structure with very small stiffness and a rather small value of  $p_0$  compared with what is applied to real structures.

### 5.3. EXAMPLE 3: CLAMPED SQUARE SANDWICH PLATE BY CHATE *ET AL.* (1995)

A clamped square sandwich plate as in Chate *et al.* (1995) was analysed, for the following data: plate frequency  $f = 52.6$  Hz, the mass of this plate  $M = 116.25$  kg.

Simplifying the plate to a one-dimensional problem, we can estimate the structural stiffness from the frequency and mass; the stiffness  $K$  then becomes 321 635 N/m and we use  $A_f = 1$  m<sup>2</sup>. Now we add an explosive charge of  $Q = 400$  kg at a distance of  $R_r = 50$  m and a cut-off time  $T = 0.0015$  s. The density of water is set to  $\rho = 1000$  kg/m<sup>3</sup> and the speed of sound in water to  $c = 1500$  m/s. All these values are realistic and could, for example, be applied to the hull planting in a Mine Counter Measure Vessel built in fibre reinforced plastic, FRP-sandwich.

Compared with the previous example this is a very light and stiff structure and a more realistic explosive charge and distance is used, that could be applied to real structures. The parameters for the cavitation models are chosen as before, i.e.  $\beta = 0.05$ ,  $p_v = 0.001$  MPa and  $p_\infty = -0.05$  MPa for cavitation growth and 0.10 MPa for cavitation closure.

The times of the reloading and the fluid velocity at impact for the different cases are summarized in Table 2. From Figure 7, it can be seen that both the RWM and SCM follow the DC to the time for reloading. The fluid, for the RWM, will impact the structure with a "high" velocity and cause a maximum displacement to occur after the reloading, while the SCM gives a much smaller impact pressure and the velocity of the structure is not significantly changed. Therefore, the maximum displacement occurs before the reloading, as for the DC. The PC have a smaller maximum displacement due to the fact that the  $\rho c$  damper starts to act on the system after reloading and this occurs at an earlier time.

TABLE 2  
Reloading time and fluid velocity

Minimum $p_\infty$ (MPa)	Displacement criterion (DC)		Pressure criterion (PC)		Rigid wall model (RWM)		Spherical cavity model (SCM)	
	Time (s)	Fluid vel. (m/s)	Time (s)	Fluid vel. (m/s)	Time (s)	Fluid vel. (m/s)	Time (s)	Fluid vel. (m/s)
-0.01	—	—	—	—	0.0077	1.27	0.0077	0.36
-0.05	0.0176	0.08	0.0045	0.13	0.0113	3.43	0.0113	0.97
-0.10	—	—	—	—	0.0148	5.37	0.148	1.51

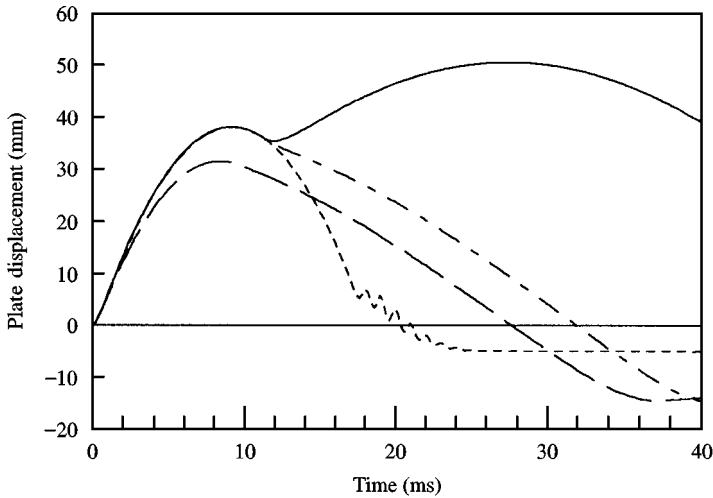


Figure 7. Plate displacement time history for cavitation models: - - - -, displacement criterion (DC); — · — ·, pressure criterion (PC); —, rigid wall model (RWM); · · · · ·, spherical cavity model (SCM).

#### 5.4. EXAMPLE 4: SANDWICH PLATE

The effect of the surrounding pressure is investigated on the same sandwich plate as in Example 3. The parameters for the cavitation models are chosen as before, ie.  $\beta = 0.05$ ,  $p_v = 0.001$  MPa and  $p_\infty = -0.01$ ,  $-0.05$  and  $-0.10$  MPa for cavitation growth and  $0.10$  MPa for cavitation closure.

The driving pressure for the growth of the cavitation causes a significant difference in the time for the reloading and the impact velocity, as can be seen in Table 2. How this affects the response of the structural displacement is shown in Figures 8 and 9.

From both Figures 8 and 9, it can be seen that the higher surrounding pressure  $p_\infty$  will cause a reloading at an earlier time and this will have a greater effect on the structural response. If the structure has a velocity in the same direction or very small velocity in the opposite direction of the fluid, the impact will increase the structural displacement. For both the RWM and SCM the reloading occurs at a later time when  $p_\infty = -0.10$  MPa. Even though the impact pressure is larger than for the other cases, the maximum structural

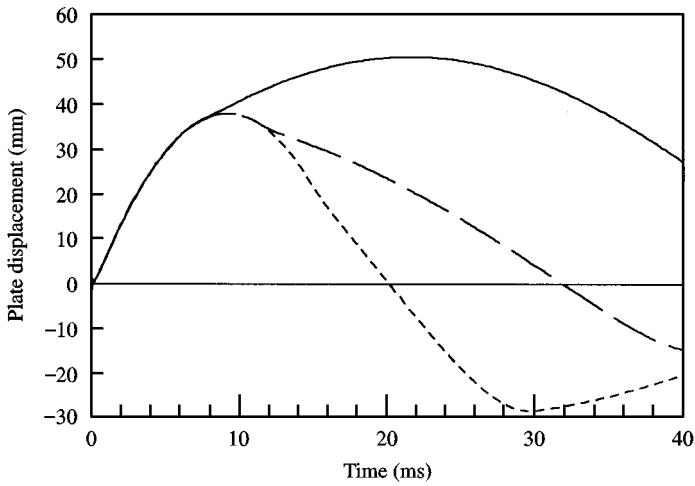


Figure 8. Plate displacement time history for the SCM: —,  $p_{\infty} = -0.01$  MPa; - - -,  $p_{\infty} = -0.05$  MPa; - · - ·,  $p_{\infty} = -0.10$  MPa.

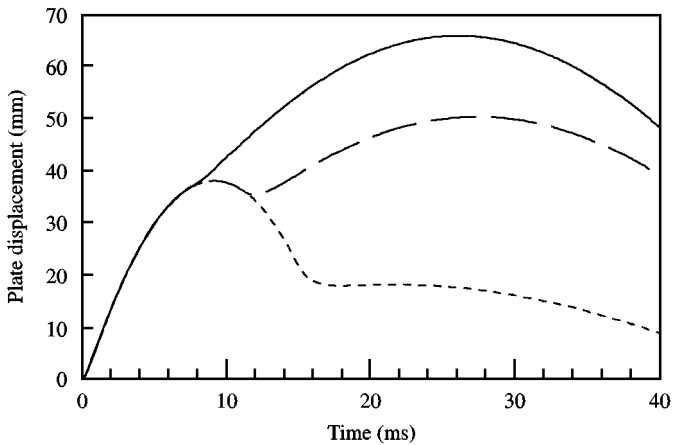


Figure 9. Plate displacement time history for the RWM: —,  $p_{\infty} = -0.01$  MPa; - - -,  $p_{\infty} = -0.05$  MPa; - · - ·,  $p_{\infty} = -0.10$  MPa.

displacement is not affected due to the fact that the structure has a larger velocity in the opposite direction.

Figure 10 shows the structural displacement for the RWM but using the slamming function for reloading, equation (15) instead of equation (14) that is otherwise used. Thus, comparing Figures 9 and 10 we can see that the impact force from the slamming is smaller and much more spread in time because the maximum displacement occurs later in time and is less than for the reloading with the function for the initial shock wave. Again, it can be seen that the magnitude of the impact is not that important; it is when the impact occurs that is important for the response of the structure.

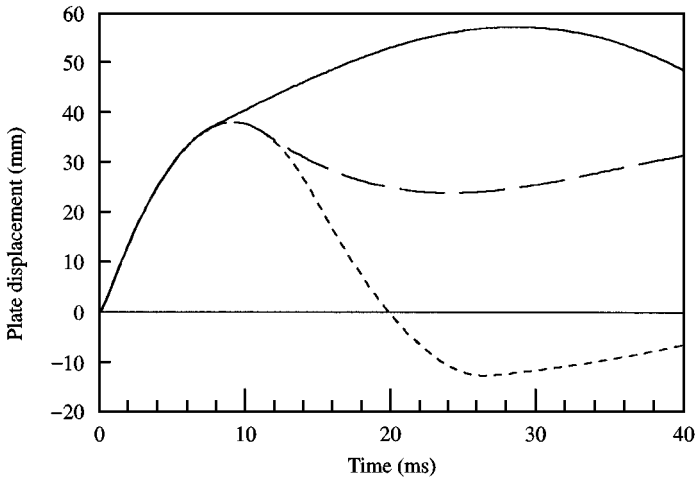


Figure 10. Plate displacement time history for RWM with slamming impact: —,  $p_{\infty} = -0.01$  MPa; — — —,  $p_{\infty} = -0.05$  MPa; - - - -,  $p_{\infty} = -0.10$  MPa.

The empirical equation (15), and especially the definition of the period  $T$ , are based on experimental results from rather small flat panel tests and this may introduce errors in using the model. If that period were shorter, the response would be very similar to the response of the spherical cavity given in Figure 8.

## 6. CONCLUSIONS

Considering a simple example, the plane wave approximation has been shown to give good results for shock-loaded structures when compared with analytical results. When it comes to the response of structures exposed to plane pressure waves including cavitation, there is no unique solution to the problem yet, and different models are used for different situations. However, a couple of models that are commonly used in practical design of structures for these types of loads have been used. These models, and two others, have been compared in an example with an infinite plate and a simplified model of a sandwich plate from the hull of a marine vessel.

Of the two most used models for practical design, the pressure criterion (PC) is the model that represents the physical phenomenon best. Both the displacement criterion (DC) and PC are used for their simplicity. If the two cavitation models rigid wall model (RWM) and single spherical cavity model (SCM) are compared, the RWM gives a higher fluid velocity but the time for reloading is almost the same. The effect of changing  $\beta$ , the volumetric fraction of cavities, or the vapour pressure inside the cavity is the same for the two models and will not significantly affect the time for the reloading.

The results of this investigation indicate that the most important factor for the impact pressure on the structure is the driving pressure for the growth of the cavity. However, for the structural response, the time for the reloading is very important, i.e. the sign of the structural velocity compared with the impact velocity of the fluid. If they are acting in the same direction, the forces are added and the structural response will be significantly affected.



Since there is no unique solution for this very complex problem, these models need to be applied and calibrated to experimental results in order to obtain numerical values for the different parameters that are needed as input in the equations.

## REFERENCES

- BARK, G. 1995 Personal communication. Chalmers University of Technology, Göteborg, Sweden.
- BLEICH, H. H. & SANDLER, I. S. 1970 Interaction between structures and bilinear fluids. *International Journal of Solids and Structures* **6**, 617–639.
- CHATE, A., RIKARDS, R., MÄKINEN, K. & OLSSON, K. -A. 1995 Free vibration analysis of sandwich plates on flexible support. *Mechanics of Composite Materials and Structures* **2**, 1–18.
- CHUANG, S. L. 1966 Experiments on flat-bottom slamming. *Journal of Ship Research* **10**, 10–17.
- COLE, R. H. 1948 *Underwater Explosions*. Princeton, New Jersey: Princeton University Press.
- DiMAGGIO, F. L., SANDLER, I. S. & RUBIN, D. 1981 Uncoupling approximations in fluid–structure interaction problems with cavitation. *Journal of Applied Mechanics* **48**, 753–756.
- DRIELS, M. R. 1980 The effect of non-zero cavitation tension on the damage sustained by a target plate subject to an underwater explosion. *Journal of Sound and Vibration* **73**, 533–545.
- FELIPPA, C. A. & DERUNTZ, J. A. 1984 Finite element analysis of shock-induced hull cavitation. *Computer Methods in Applied Mechanics and Engineering* **44**, 297–337.
- GEERS, T. L. 1974 Shock response analysis of submerged structures. *The Shock and Vibration Bulletin* **44**, 17–32.
- HANDLETON, R. T. 1985 Analysis of cavitation caused by shock wave interaction with a restrained mass. *The Shock and Vibration Bulletin* **55**, 193–203.
- MILLER, R. D., LEV, A. & AMIR, G. G. 1991 Shock analysis of ship structures due to underwater explosions using HULLCAV3/NASTRAN and HULLCAV3/DYNA approaches. *Proceedings of the sixty second Shock and Vibration Symposium*, vol. 2, Springfield, Virginia, U.S.A.
- MINDLIN, R. D. & BLEICH, H. H. 1953 Response of an elastic cylindrical shell to a transverse step shock wave. *Journal of Applied Mechanics* **20**, 189–195.
- MØRCH, K. A. 1982 Energy considerations on the collapse of cavity clusters. *Applied Scientific Research* **38**, 313–321.
- MØRCH, K. A. 1989 On cavity cluster formation in a focused acoustic field. *Journal of Fluid Mechanics* **210**, 57–76.
- MOYER, T. 1995 Personal communication. NKF Engineering, INC, Arlington, Virginia, U.S.A.
- MOYER, T., AMIR, G. G., OLSSON, K. -A. & HELLBRATT, S. -E. 1992 Response of sandwich structures subjected to shock loading. *Proceedings of the Second International Conference on Sandwich Construction*, 9–12 March, Gainesville, Florida, U.S.A.
- TAYLOR, G. I. 1941 *The Pressure and Impulse of Submarine Explosion Waves on Plates*. Cambridge: Cambridge University Press.